PERGAMON

Mechatronics 11 (2001) 1–12

MECHATRONICS

A bandpass filter-based approach to crop row location and tracking

T. Hague*, N.D. Tillett

Silsoe Research Institute, Wrest Park, Silsoe, Bedfordshire, NK45 4HS, UK

Received 11 July 1999; received in revised form 4 January 2000; accepted 19 January 2000

Abstract

A method of locating crop rows in image sequences is described. Unlike several previously reported algorithms, the method does not rely upon the segmentation of plant material from the background on the basis of absolute brightness or colour. Rather, the periodic amplitude variation due to parallel crop rows is exploited. Given the geometry of the camera arrangement and the crop row spacing, a filter is derived which allows the crop rows to be extracted whilst attenuating the effects of partial shadowing and spurious features such as weeds. The position and orientation of the rows are tracked using an extended Kalman filter.

The method has been used to guide a mechanical hoe in winter wheat with an RMS positional error of 15.6 mm at a speed of 1.6 ms^{-1}, despite the presence of complex shadows cast by the tractor in the imaged area.

Keywords: Bandpass filter; Kalman filter; Guidance; Tracking; Crop rows

1. Introduction

Weed control by inter-row cultivation in cereal crops requires the position of the hoe tines to be controlled with an accuracy greater than that of manually driven tractor. A possible solution to this problem is to provide a

* Corresponding author. Tel.: +44-1525-860000; fax: +44-1525-860156.

0957-4158/01/$ - see front matter
PII: S0957-4158(00)00003-9

self aligning hoe, which automatically detects the location of the crop rows, and adjusts the lateral position of the cultivators to compensate for driver error.

In our previous work [1] a trial system was described which used analysis of video images to determine the offset of the hoe, and generate control signals for a hydraulic side-shift mechanism in order to correct any error. The system was shown to perform adequately under uniform lighting conditions; however, operation was not possible with partial shadowing of the image area because the image analysis method was dependent upon a simple binary threshold applied to the near-IR image to discriminate plant material from the background. This is a significant limitation, since the tractor and the hoe itself frequently cast shadows onto the imaged area. Many other reported methods also rely upon the derivation of a binary (crop plant/not crop plant) classification of a grey scale [2,3] or colour [4] image by thresholding; these methods may be expected to exhibit similar problems in the presence of partial shadow.

Whilst it is possible to contrive mechanical solutions to the problems of partial shadow in images, such as the use of shading [5] or the use of multiple camera views, these methods result in a more cumbersome and expensive machine. A more desirable approach is to devise image analysis techniques more robust to variable illumination.

The approach adopted here was partially inspired by template matching methods, such as that used by Fukuda et al. and Abe et al. [6,7] to locate air conditioning fittings. The use of positive and negative templates to match dark and light patterns in the image is a valuable concept, since in the later stages of crop development, it is the dark areas of exposed soil which provide the strongest indications of row location.

Olsen [8] describes two methods of crop row location. Both methods determine lateral offset of the rows from a plan view image in which the crop rows are near parallel with the image y-axis. The image is reduced to a single line by summation of pixel intensities in each column of the image. The first method proceeds by fitting a sinusoid to the summed intensities; this method offers robustness to missing parts of the crop row pattern. The second method applies a Butterworth low pass filter to smooth the summed intensities; local maxima in the filtered intensity are then taken to be the location of the crop rows. This second method was found to be relatively insensitive to shadowing.

We describe a unified approach which combines the benefits of the two methods of Olsen, i.e., robustness to missing parts of the planting pattern and variable illumination. The basis of the approach is to detect the periodic component in the amplitude of scan lines of the image due to the crop rows. Given that the row spacing on the ground and the geometry of the optical arrangement are known, the period in image pixels can be computed for a given line in a perspective image of the crop. A bandpass filter matched to the crop row spacing is constructed in the frequency domain; this is then transformed into a template in the space domain which is matched against the image scan lines by convolution. This is

done for a set of scan lines evenly spaced in the image; a Kalman filter [9,10] then uses the observations derived to track the lateral offset and orientation of the crop rows.

2. Experimental apparatus

The apparatus used in the previously reported trials [1] was used again here without modification. The machine is operated in a field of winter wheat; there were a moderate level of weeds present, and straw from the previous crop. The only unusual feature of the crop is that it was drilled on a wider spacing than is customary to permit hoeing. This increased spacing of 220 mm compared with the traditional 125 mm has been shown [11] to have no significant detrimental effect on yield.

Images are taken from a video camera mounted at a height of 1.2 m directly above a crop row to the left side of the tractor and inclined at 45°. This positioning permits a view of around 2.5 m length of five rows of crop. Also visible in the image are the tractor wheel and part of the hoe mechanism.

A standard CCD camera is used, which is sensitive in the near infra-red; a filter is fitted to block visible light. Images from the camera are digitised and processed at frame rate (25 frames/s) using an 8-bit grey scale and a resolution of 192×144 pixels. All processing is performed by a 200 MHz Pentium-based computer mounted in the tractor.

2.1. Optical arrangement

Fig. 1a shows the arrangement of the camera over the crop rows. The coordinate frame (x_w, y_w) has its origin at the intersection of the optical axis of the camera and the ground plane. Let the location (x_w, y_w) correspond to location (x_u, y_u) on the image plane. Using a pinhole camera model and neglecting radial lens distortion,

$$\frac{x_u}{f} = \frac{x_w}{z + y_w \sin \phi} \tag{1}$$

$$\frac{y_u}{f} = \frac{-y_w \cos \phi}{z + y_w \sin \phi} \tag{2}$$

Note that y_u increases down the image as is conventional for image coordinate systems.

From Fig. 1b, the crop rows are described by the relationship:

$$x_w = x_h + (d + y_w) \tan \psi \tag{3}$$

where x_h and ψ are the lateral position of the hoe blades and the heading angle and d is the constant distance of the hoe tines behind the centre of the image.

Substituting for x_w, y_w in Eq. (3) using Eqs. (1)–(2) yields:

$$x_u = \frac{y_u}{z \cos \phi}[(x_h + d \tan \psi) \sin \phi - z \tan \psi] + \frac{f}{z}[x_h + d \tan \psi] \tag{4}$$

Finally, the pixel coordinates (x_i, y_i) in the captured image are computed by scaling for the CCD cell pixel dimensions (d_x, d_y), and translating by half the image dimensions (I_x, I_y) such that the origin is at the conventional top left location:

$$x_i = \frac{x_u}{d_x} + \frac{I_x}{2} \tag{5}$$

$$y_i = \frac{y_u}{d_y} + \frac{I_y}{2} \tag{6}$$

Eqs. (4)–(6) provide the basis for the extended Kalman filter (EKF) observation model.

Combining Eq. (1) and Eq. (2) yields:

$$x_u = x_w\left(\frac{y_u \tan \phi + f}{z}\right) \tag{7}$$

Assuming that the heading angle ψ remains small, the crop row spacing x_r in

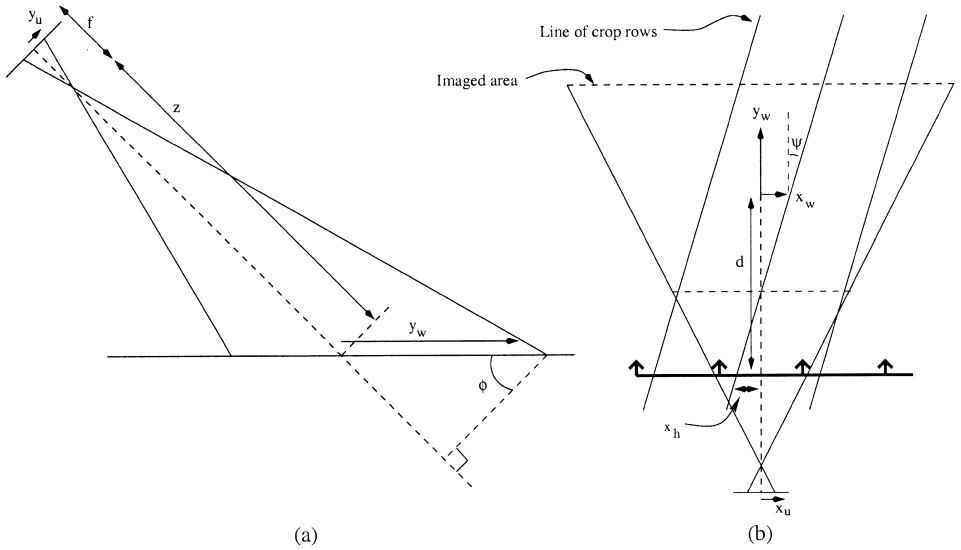

Fig. 1. Pinhole camera model (not to scale): (a) side elevation; (b) plan.

image pixels for a given row spacing r on the ground at any horizontal line y_u in the image may be calculated:

$$x_r \approx \frac{r}{d_x}\left(\frac{y_u \tan \phi + f}{z}\right) \tag{8}$$

The parameters f, z, ϕ, d_x, d_y are obtained by a calibration procedure. For the camera and digitising hardware used in our implementation, it is known that $d_x = d_y$. Further, the effective focal length f and the pixel dimensions are linearly dependent, so d_x, d_y can be given an arbitrary value. The other parameters are determined using a calibration image consisting of a 220-mm grid of black disc features on a white background set on the ground plane; the values of f, z and ϕ are found by a least squares technique. This method also yields the RMS residual error in the calibration grid points; this was found to be a little less than one pixel, illustrating that lens distortions can be safely neglected.

3. Bandpass filter design

A filter is required to extract, from a scan line of the image, the periodic component of the image intensity due to the crop rows. A bandpass filter is used, matched to the crop row spacing. The high frequency cut off serves, as in the second method of [8], to attenuate the effects of spurious features such as weeds and detail of the internal structure of the crop row. The additional low frequency cut off is used to suppress the effect of illumination variation over the field of view. The filter must not introduce a phase shift, since this would lead to error in offset. Since the entire image is held in memory, the filter need not be constrained by causality, and thus the design is straightforward.

Let x_r be the period in pixels of the component of the image due to the crop rows, calculated for a given scan line using the pinhole camera model. The required angular frequency of the centre of the passband is thus

$$\omega_c = \frac{2\pi}{x_r}$$

In practice, the observed period will vary slightly as a result of a combination of error sources. Significant sources include inaccuracies in the drilling of the crop, variation in the camera inclination as a result of imprecise adjustment of the implement mounting on the tractor's three point hitch, and variation in crop height with normal growth. To allow for these variations, the filter is given a passband as shown in Fig. 2. The passband width of $2\,\omega_b$ is arrived at based upon an estimate of $\pm 15\%$ of the nominal row spacing for the likely magnitude of the combined sources of error listed above; this corresponds approximately to $\omega_b = 0.15\,\omega_c$ in the frequency domain.

The desired filter response is thus:

$$F(\omega) = \begin{cases} 1 & \text{if } \omega_c - \omega_b \leq |\ \omega\ | \leq \omega_c - w_b \\ 0 & \text{otherwise} \end{cases}$$

Applying the Fourier inverse cosine transform gives:

$$\begin{aligned} f(x) &= \mathscr{F}^{-1}(F(\omega)) \\ &= \sqrt{\frac{2}{\pi}} \int_0^{\infty} F(\omega) \cos\ \omega x\, d\omega \\ &= \sqrt{\frac{2}{\pi}} \int_{\omega_c - \omega_b}^{\omega_c + \omega_b} \cos\ \omega x\, d\omega \\ &= \frac{2}{x} \sqrt{\frac{2}{\pi}} [\cos(\omega_c x) \sin(\omega_b x)] \end{aligned}$$

To implement the filter, the horizontal line in the image is convolved with $f(x)$. As a matter of computational convenience, this convolution is performed using integer arithmetic. Since the requirement is to find the offset, in image pixels, of the peak corresponding to the central crop row, an arbitrary scaling of $f(x)$ can be applied to give a convenient magnitude; we have chosen to use an 8-bit scale. The maximum value of $f(x)$ is when $x \to 0$:

$$\lim_{x \to 0} f(x) = 2\omega_b \sqrt{\frac{2}{\pi}}$$

Thus, the tabulated filter function is:

$$\tilde{f}(x) = \frac{127}{\omega_b x} [\cos(\omega_c x) \sin(\omega_b x)]$$

A further issue is that in practice, $\tilde{f}(x)$ cannot be tabulated over an infinite domain. Neither is it necessary, since the physical constraints on the imaged area mean that five crop rows are visible, and thus only five cycles of the filter's input signal are available. Accordingly, the filter is truncated to $\pm 9x_r/4$. The resulting

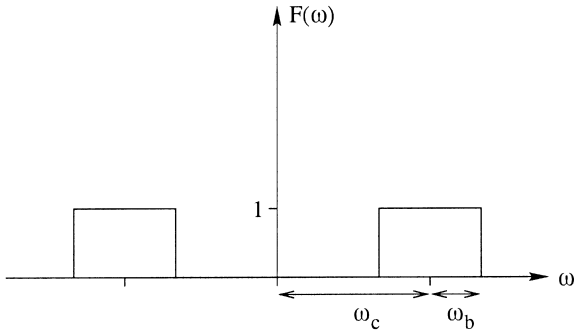

Fig. 2. Desired filter response for row finding.

filter profile is shown in Fig. 3. In this case, the period $x_r = 29$ pixels, and $\omega_b = 0.15\ \omega_c$.

Considering $\tilde{f}(x)$ as a template for matching crop rows, it can be seen to have desirable properties; that it takes negative values between the rows allows the dark areas of exposed soil to contribute information as well as the bright crop rows. The weighting towards the central peak reflects to the increased uncertainty in position of the outlying rows due to potential variability in row spacing.

A fixed set of horizontal scan lines in the image are used for row finding (eight are used in the current implementation). For these lines, Eq. (8) is used to compute the apparent row spacing in image pixels. Using this value of x_r, a bandpass filter function is tabulated as an initialisation step, using Eq. (3). As each image is captured, the filter is applied to each of the lines. Since a Kalman filter approach has been adopted for combining the observations with a prior prediction, the expected location of the crop rows is known. Thus it is only necessary to find the maximal value of the filtered image scan line over $\pm x_r/2$ pixels of the expected value; this much reduces the computational burden of the required convolution operation.

4. Kalman filter implementation

The x coordinates so found are then used as observations for a Kalman filter. The three element state vector $\mathbf{x} = [x_h\ \theta\ \alpha]^T$ is estimated, where x_h is the lateral offset of the tines and θ is the orientation of the rows. In practice, mounting of the camera such that it is correctly oriented proves difficult, and a small

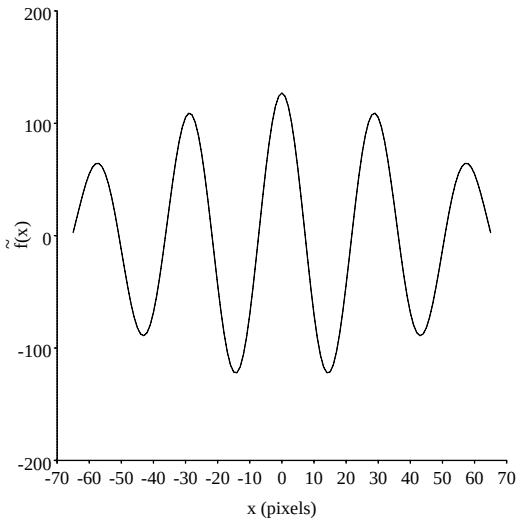

Fig. 3. The tabulated filter function, scaled for 8-bit magnitude.

orientation bias might result from this misalignment. This has an unacceptable effect on the estimation of tine location. The solution adopted here is to correct this by including the bias α as a state to be estimated.

4.1. Process model

The process model used is unchanged from the form used in [1], and is thus simply summarised here.

The model combines the kinematic constraint of the tractor on which the hoe is mounted, and an input vector $\mathbf{u}(k) = [s(k)\ y(k)]^T$ consisting of the forward speed $s(k)$ (measured odometrically) and incremental motion of the hoe side shift mechanism $y(k)$ (measured by an LVDT). Following the notation of [10], the prediction takes the form:

$$\hat{\mathbf{x}}(k+1 \mid k) = \mathbf{f}(\hat{\mathbf{x}}(k \mid k), \mathbf{u}(k))$$

where

$$\mathbf{f}(\mathbf{x}(k), \mathbf{u}(k)) = \begin{bmatrix} x_h(k) + \tau s(k)\theta(k) + y(k) \\ \theta(k) \\ \alpha(k) \end{bmatrix}$$

and τ is the time interval between predictions (i.e., 40 mS).

The predicted state covariance is computed using a first-order approximation:

$$\mathbf{P}(k+1 \mid k) = \mathbf{F}_{\mathbf{x}}\mathbf{P}(k \mid k)\mathbf{F}_{\mathbf{x}}^T + \mathbf{F}_{\mathbf{u}}\mathbf{Q}(k)\mathbf{F}_{\mathbf{u}}^T + \mathbf{N}(k) \tag{9}$$

where $\mathbf{F}_{\mathbf{x}} = \frac{\partial \mathbf{f}}{\partial \mathbf{x}}$, $\mathbf{F}_{\mathbf{u}} = \frac{\partial \mathbf{f}}{\partial \mathbf{u}}$ evaluated at $\mathbf{x} = \hat{\mathbf{x}}(k \mid k)$, $\mathbf{u} = \mathbf{u}(k)$. The first term on the right side of Eq. (9) relates to the propagated variance from the previous time step. The input $\mathbf{u}(k)$ is modelled as uncertain with variance $\mathbf{Q}(k)$, the magnitude of which is derived from the sensor specifications. The final term $\mathbf{N}(k)$ represents the uncertainty due to unmodelled disturbances in the prediction process, namely tractor driver error, row curvature and side slip.

4.2. Observation model

Eight observations are generated by filtering lines of the image and locating the amplitude peak due to the central crop row. The observation model allows the lateral offset of these peaks in the image to be used to update the state vector. It is assumed that the observation noise is not correlated between observations, and thus they may be processed sequentially.

Let $\psi = \theta + \alpha$, i.e., modelling the observed row orientation as the true orientation plus some constant camera skew error also to be estimated. From the pinhole camera model, Eqs. (4)–(6) can be rearranged into the form

$$x_i = h(\mathbf{x}, y_i) \tag{10}$$

For each horizontal image line y_i, the predicted image feature position $\hat{x}_i$ is computed. The image line is then filtered, as described above, and searched over the range $[\hat{x}_i - \frac{x_r}{2}, \quad \hat{x}_i + \frac{x_r}{2}]$ to find the actual lateral position of the central row, x_i. To improve robustness to erroneous observations, the observation is validated against the prediction using Mahalanobis distance, and accepted if

$$(x_i - \hat{x}_i)^T(\mathbf{HP}(k+1 \mid k)\mathbf{H}^T + R(y_i))^{-1}(x_i - \hat{x}_i) < \chi^2 \tag{11}$$

where $\mathbf{H} = \frac{\partial h}{\partial x}$ evaluated at $\mathbf{x} = \hat{\mathbf{x}}(k+1 \mid k)$, χ^2 is a 1 d.o.f. chi squared value corresponding to a 95% confidence interval; observations falling outside this interval are rejected as unlikely to be valid. $R(y_i)$ is the observation variance; this is a function of y_i as it is assumed that the variance of the observations is constant in *ground coordinates*, thus in the perspective view of the camera, it is dependent upon image ordinate. Should the observation be accepted, the innovation is incorporated into the state estimate using the standard first order EKF update equations.

5. Hoe control

The hoe side shift mechanism is operated in a bang–bang fashion, on the basis of the estimated offset x_h. The hydraulic cylinders are driven in such a direction as to reduce the offset whenever the estimated offset exceeds a dead band of ± 9 mm.

6. Experimental results

In addition to use in agronomic trials [12], the performance of the experimental hoe system has been evaluated using a 0.5-ha trial plot of winter wheat at Silsoe, UK (approximate location 52°1′N, 0°24′W). The particular results presented here were obtained at approximately 4:15 pm on 12 August 1998 in clear conditions. The crop rows were aligned in an east–west direction. These circumstances were selected to exhibit strong shadows. At the time of the trial, the crop was approximately 150 mm high. The tractor was driven at approximately 1.6 ms^{-1}.

For evaluation purposes, the software was configured to keep a stored record of each frame of video processed for up to 30 s of operation. For each frame, the individual observations used by the Kalman filter (i.e., the location of the peak in the eight filtered image lines) were marked in the image with crosses, and the recovered location of the rows was recorded by drawing lines at the estimated location of the three central rows.

Arbitrarily selected images representative of the conditions can be seen in Fig. 4. In fig. 4a, the tractor was heading towards the west, and the image area is uniformly lit by direct sunlight. These are the conditions under which the earlier method reported in [1] was evaluated. In Fig. 4b, the tractor was heading towards

the east. Under these conditions the shadow of both the tractor and the hoe are cast into the imaged area. As can be seen, the crop rows are still correctly located. The method of [1], because of its reliance upon binary thresholding, could not achieve a successful result under these conditions. It is under the conditions seen in Fig. 4b that the following trial was conducted.

To record the actual offset of the hoe, one of the hoe tines was removed, and replaced by a nozzle which dispensed a trace of paint. The overall performance of the system was assessed by measuring the location of the trace relative to the crop rows. To facilitate the measurement, a measuring aid marked at intervals equal to the row spacing was used; these marks were aligned with the crop rows. A second scale was used to read the offset of the paint trace from the central position to the nearest 5 mm.

Before the trial commenced, manual adjustment was made to null any constant

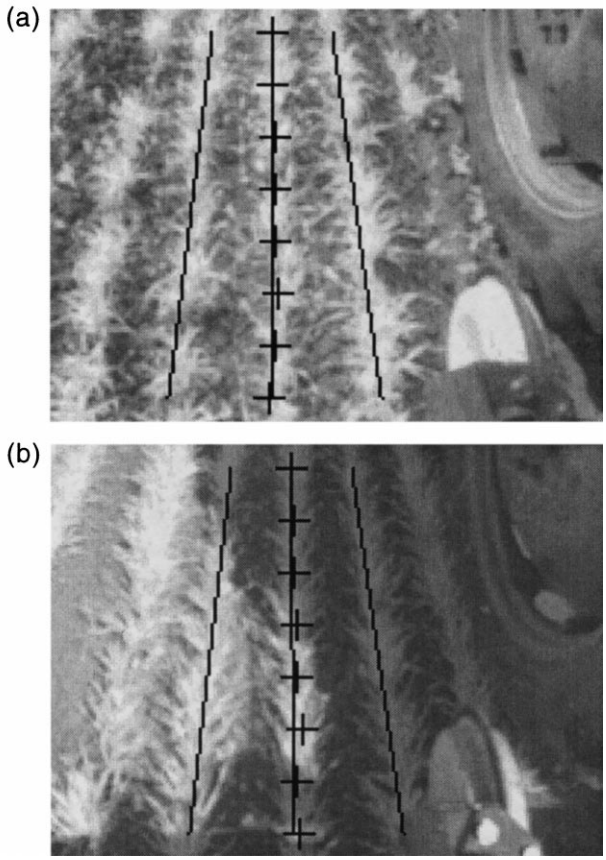

Fig. 4. Row location: (a) uniform lighting conditions; (b) with deep shadows.

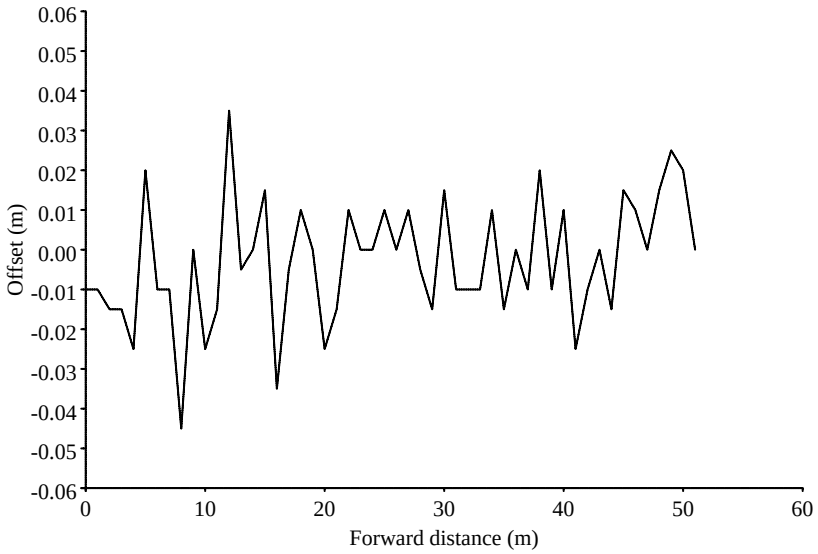

Fig. 5. Measured hoe lateral position offset.

bias of the hoe tines. A pass of approximately 50 m length was performed, and the hoe offset measured at 1 m intervals following the procedure described above. The measured offsets are recorded in Fig. 5. An analysis of the measurements shows a residual bias of 2.9 mm and an RMS error of 15.6 mm.

7. Conclusions

It has been demonstrated that the algorithm described is capable of reliably tracking the location of a set of crop rows in the presence of severe shadows in the camera field of view. This significantly increases the range of operating conditions which may be tolerated when compared with the previously reported method.

The measured RMS error in hoe positioning during a trial under difficult illumination conditions was 15.6 mm, only marginally poorer than the RMS errors in the range 11–14 mm attained by the previous method under ideal lighting conditions. These figures, of course, include the errors inherent in the manual measurement (to the nearest 5 mm) of the trace. Moreover, a significant component of the error is due to the hydraulic control, the current implementation of which has a ± 9 mm dead band. It is thought that an accuracy of ± 25 mm or better is required to avoid crop damage; 94% of the offset measurements in this trial fall within that interval.

As part of the experimental method, any constant bias in hoe offset was

manually nulled before the trial. This offset has two sources. The first is mechanical misalignment of the camera in the lateral direction, and only requires adjustment when the position of the camera and tines on the hoe frame have been disturbed, and is therefore unimportant. However, a second source of bias is observed when the sun is low in the sky, and the crop rows are illuminated from one side. These conditions may cause biased estimation of the row location. Further work is needed to quantify this; the use of colour techniques may be necessary to reduce or eliminate the effect.

Acknowledgements

This work was funded by the Ministry of Agriculture, Fisheries and Food, as part of a joint research programme with IACR Long Ashton and ADAS Boxworth. Additional support was provided by Garford Farm Machinery and Keith Rennie Machinery Ltd.

References

[1] Tillett ND, Hague T. Computer vision based hoe guidance for cereals — an initial trial. J Agric Eng Research 1999;74(3):225–36.
[2] Marchant JA. Tracking of row structure in three crops using image analysis. Computers and Electronics in Agriculture 1996;15(2):161–79.
[3] Reid JF, Searcy SW. An algorithm for separating guidance information from row crop images. Trans of the ASAE 1988;13(6):1624–32.
[4] Billingsley J, Schoenfisch M. The successful development of a vision guidance system for agriculture. Computers and Electronics in Agriculture 1997;16(2):147–64.
[5] Slaughter DC, Chen P, Curley RG. Computer vision guidance system for precision cultivation. In: ASAE Annual International Meeting, Minneapolis, August, 1997 Paper no. 97–1079.
[6] Fukuda T, Yokoyama Y, Arai F, Abe Y, Tanaka K. Navigation system based upon ceiling landmark recognition for autonomous mobile robot-position/orientation control by landmark recognition with plus and minus primitives. In: IEEE International Conference Robotics and Automation, 1996. p. 1720–5.
[7] Abe Y, Shikano M, Fukuda T, Arai F, Tanaka Y. Vision based navigation system by variable template matching for autonomous mobile robot. In: IEEE International Conference Robotics and Automation, Leuven, Belgium, April, 1998. p. 952–7.
[8] Olsen HJ. Determination of row position in small-grain crops by analysis of video images. Computers and Electronics in Agriculture 1995;12(2):147–62.
[9] Kalman RE. A new approach to linear filtering and prediction problems. J Basic Eng Trans ASME, series D 1960;82:35–45.
[10] Bar-Shalom Y, Fortmann T. Tracking and data association. New York: Academic Press, 1988.
[11] Blair AM, Jones P, Orson JH. Integration of row widths, chemical and mechanical weed control and the effect on winter wheat yield. Aspects of Applied Biology 1997;50:385–92.
[12] Tillett ND, Hague T, Blair AM, Jones PA, Ingle R, Orson JH. Precision inter-row weeding in winter wheat. In: The 1999 Brighton Conference — Weeds, Brighton, UK. British Crop Protection Council, 1999. p. 975–80.